ELSEVIER

Surface and Coatings Technology 79 (1996) 246–251

SURFACE & COATINGS TECHNOLOGY

The effect of microstructure on the corrosion behaviour of electroless Ni–P alloys in acidic media

T. Mimani, S.M. Mayanna *

Department of Chemistry, Central College, Bangalore University, Bangalore 560 001, India

Received 22 November 1994; accepted in final form 20 February 1995

Abstract

The structure and surface morphology of Ni–P alloys obtained by electroless plating has been analysed by X-ray diffraction and microscopic techniques respectively. The bath composition has been found to affect the microstructure of the alloy. The corrosion behaviour of these alloys in acidic media: 1 N H_2SO_4, 1 N HCl and 5% NaCl (pH 5) was investigated using electrochemical techniques. The corrosion characteristics varied with the degree of crystallinity, the composition of the alloy and the presence of inclusions in the alloy.

Keywords: Electroless; Ni–P alloys; Microstructure; Corrosion resistance

1. Introduction

Alloys are frequently used in industries to meet high strength and corrosion resistance of the base materials. Amorphous Ni–P alloys find significant commercial importance in electronic, aerospace and automotive applications [1,2]. Several studies have been made on the evaluation of corrosion resistance of these alloys prepared either by melt spinning [3] or electrodeposition techniques [4,5]. In these findings the corrosion behaviour is explained in terms of percentage of phosphorus.

The corrosion resistance of the electroless Ni–P coatings depends on several factors, namely the phosphorus content [6], degree of crystallinity, size and orientation of the grains [7], phase and structural variation and the thickness and porosity [8]. It has been established that various chemical states of Ni and P, enriched in the surface film, are responsible for the passivation process [9]. Although phosphorus in Ni–P alloys can produce both detrimental and beneficial effects, the protective effect is very much dependent on the microstructural composition.

It has been observed [10] that the plating bath components boric acid, sodium chloride, lead ions and allyl thiourea produced a considerable change in the plating rate and the composition of the alloy. Recently, the characterization of microstructure of surface coatings has been well documented [11,12] and the detailed study on such a topic is of considerable practical significance. In the present communication, the results pertaining to the effect of several components in plating bath solution on the microstructure and the corrosion resistance are reported.

2. Experimental

The Ni–P coatings (thickness 20–30 μm) were obtained on copper substrates from a bath solution (AP) of composition 0.1 M $NiSO_4 \cdot 7H_20$, 0.15 M $NaH_2PO_2 \cdot 2H_2O$, 0.8 M H_3BO_3, 0.8 M NaCl, 0.4 M $NaKC_4H_4O_6 \cdot 4H_2O$ and 3.5×10^{-5} M C_4H_7NHS at 343 K and pH 5 under the plating conditions used earlier [10]. Experiments were also carried out to get Ni–P coatings using lead ions (9.7×10^{-6} M) (PB) and a mixture of lead ions (4.35×10^{-5} M) and allylthiourea (1.75×10^{-5} M) (PL) as stabilizers. Coatings were also obtained from this bath solution without sodium chloride (BA) or boric acid (SC). The coatings obtained under different experimental conditions were investigated in detail.

The microstructural characteristics of each Ni–P coating were studied using X-ray diffractometry (PW1140/90, Philips) and scanning electron microscopy (Oxford, Link

* Author for correspondence.

SSDI 0257-8972(95)02446-8

QX 2000). Galvanostatic polarizations were carried out at ambient temperature and stirring in a three-compartment cell containing deaerated corrosive media (1 N H_2SO_4, 1 N HCl or 5% NaCl (pH 5)) using a potentiostat (362A, PG&G PAR, USA). Platinum foil and a saturated calomel electrode were used as counter and reference electrodes respectively. Experiments were repeated under each set of experimental conditions to ensure reproducibility.

3. Results

The Ni–P alloys obtained under different experimental conditions were examined for microstructural and phase characteristics by SEM/EDAX (Figs. 1 and 2) and X-ray diffraction. Fig. 3 represents the XRD patterns of the Ni–P alloys obtained from AP and PB plating baths.

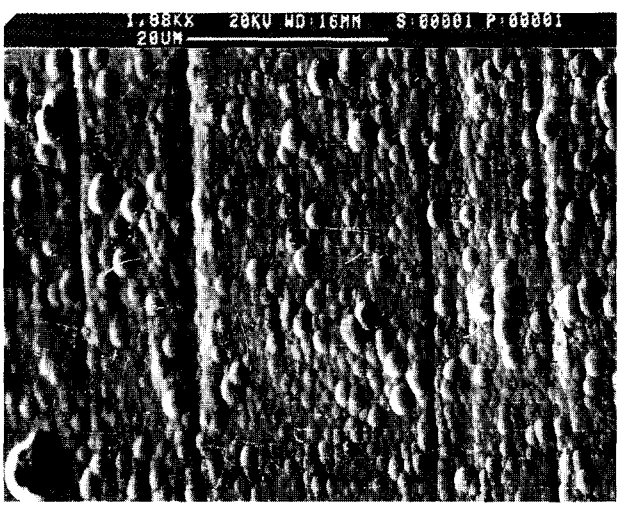

(a)

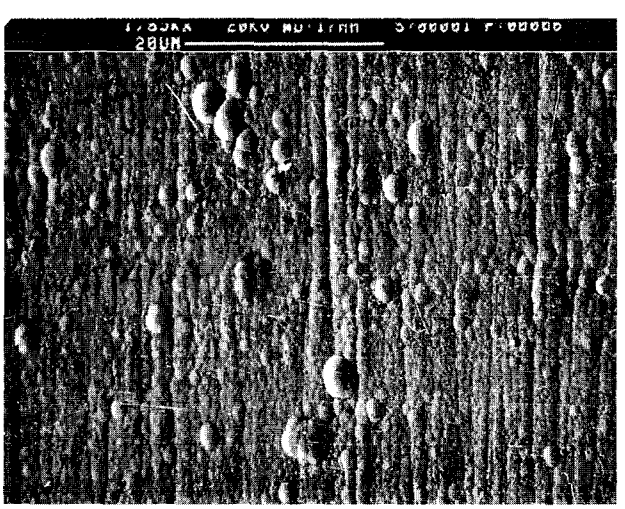

(b)

Fig. 1. Scanning electron microphotographs of the (A) AP and (B) PB coatings.

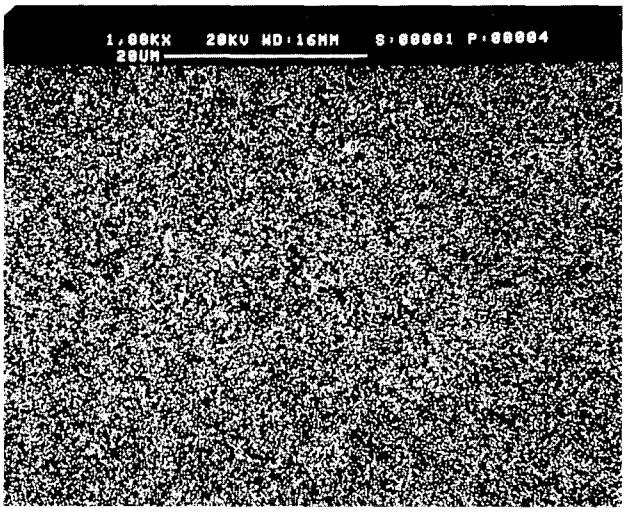

(a)

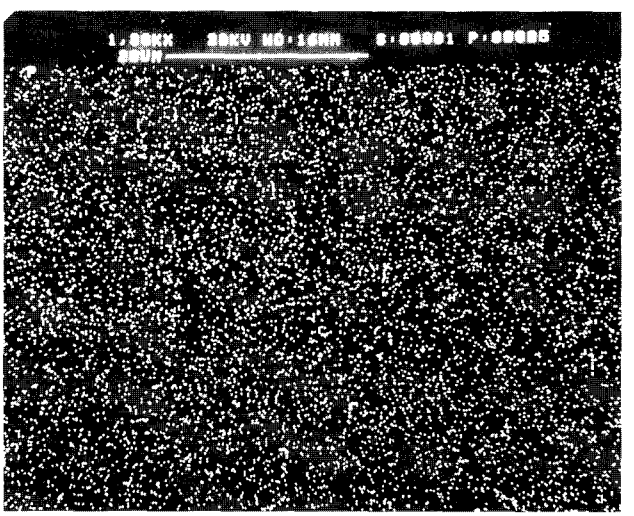

(b)

Fig. 2. The distribution of elements in AP (A) Ni and (B) P (EDAX dot mapping method).

These alloys were amorphous and they showed crystallinity on heating for 2 h under vacuum at 673 K (Fig. 4). The diffused peak height pertaining to Ni(111) varied with different coatings plated under different conditions. From the diffraction patterns, the values of full width at half-maximum (FWHM) [13], (the degree of crystallinity), were evaluated (Table 1). These values for various bath compositions are in the order

PB > AP > BA > PL > SC

The broad diffused band of PB compared with AP reflects its high amorphous nature which persists even after heat treatment. The intensities due to the Ni(111) phase were very weak compared with the Ni_3P phase (Fig. 4).

In the crystalline patterns of BA and SC, an additional peak with a lattice parameter d of 1.91 Å was noticed. Analysis of the XRD pattern shows the presence of

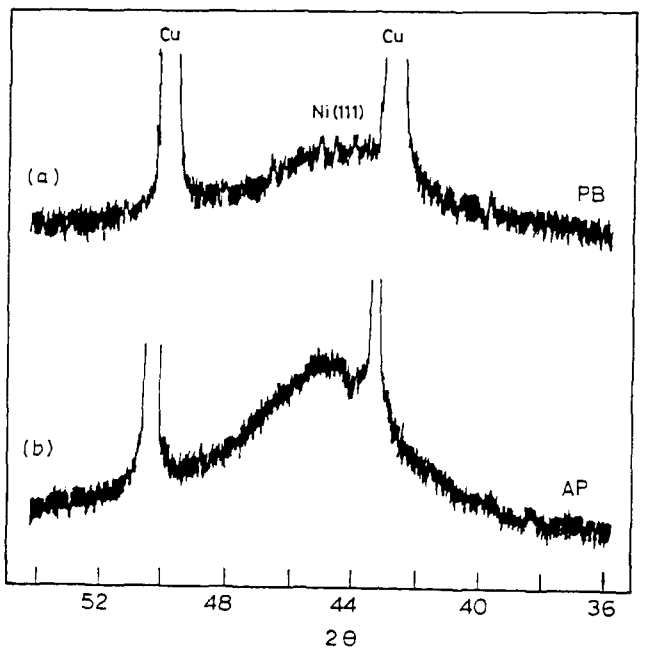

Fig. 3. X-Ray diffraction patterns of the as-plated (a) PB and (b) AP Ni–P alloys (as plated).

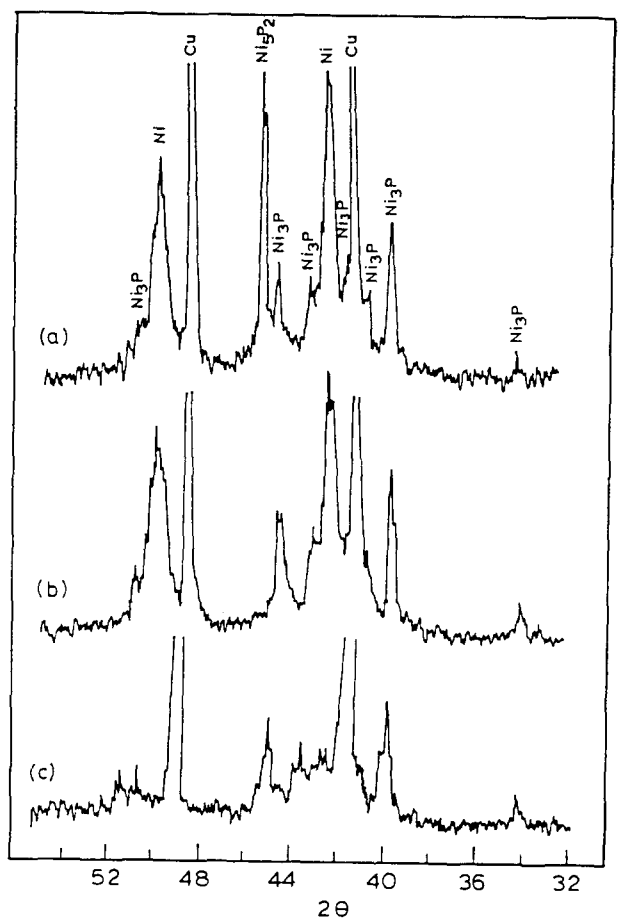

Fig. 4. XRD patterns of heat treated Ni–P alloys: (a) BA, (b) AP and (c) PB.

Table 1
The variation of plating rate, percentage of phosphorus and peak width with the bath composition

Bath type	Plating rate (mg cm $^{-2}$, 30 min)	phosphorus (wt.%)	FWHM (degree)
PB	1.3	19	8.0
AP	2.0	16	6.6
NS[a]	1.1	11	5.0
SC	1.9	9	5.8
BA	2.0	8	6.0
PL	2.8	6	5.6

[a] NS, unstirred AP bath solution.

nickel phosphide (Ni_5P_2) with a slightly distorted unit cell parameter a_0 of 13.27 Å compared with the reported value of 13.22 Å.

The structural variations in the coatings are usually related to their chemical reactivity, which can be best studied by their corrosion characteristics. Thus, in order to understand the corrosion behaviour of these coatings, detailed potentiodynamic polarization studies were made in 1 N H_2SO_4 at 303 K. The polarization diagrams (Fig. 5) were obtained by scanning the potential at a rate of 0.1 mV s^{-1} in the range ± 250 mV s^{-1} of the open circuit potential E_{corr}. From the polarization diagrams the anodic β_A and cathodic β_C Tafel slopes were evaluated.

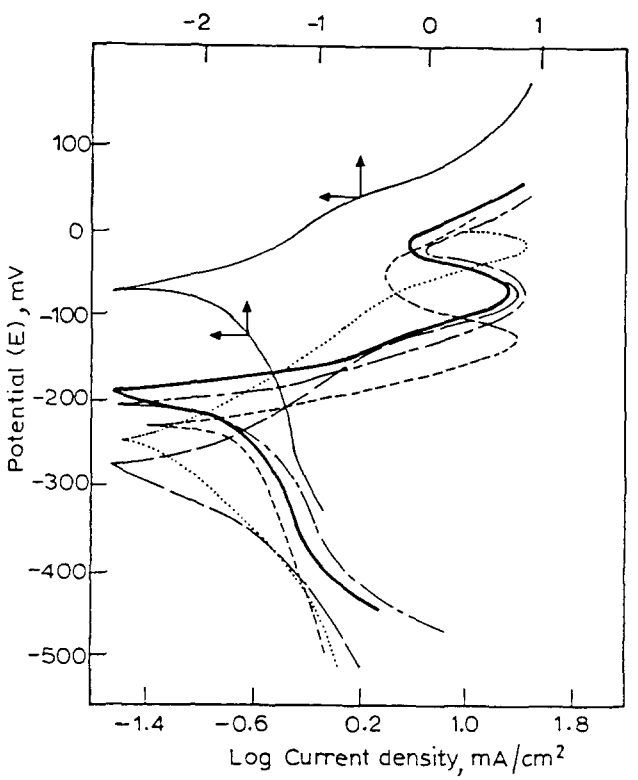

Fig. 5. Polarization pattern of the Ni–P alloys obtained under various bath compositions: (...) AP; (—) PB; ( ) SC; (- -) NS; ( ) BA and (—) PL in 1 N H_2SO_4 at 303 K.

Linear polarization experiments were also carried out by scanning the potential ±20 mV about an open circuit potential at the same rate of 0.1 mV s^{-1}. The polarization resistance values, $R_p(E/I)$ were evaluated from these plots. The corrosion current density (i_{corr} (μA cm^{-2})) was calculated using the equation

$$i_{corr} = \frac{\beta_A \beta_C}{2.303 R_p(\beta_A + \beta_C)} \quad (1)$$

The rate of corrosion (R_{mpy}) was evaluated using the relation [14]

$$R_{mpy} = 0.13ie/\rho \quad (2)$$

where i is the current density, e is the equivalent weight (chemical), while ρ is the density of the alloy. The corrosion data of the coatings in 1 N H_2SO_4 are supplemented in Table 2. The values of i_{corr} of the deposits are in the order:

SC > BA > AP > PL > PB

The anodic Tafel slope ranges from 50 mV dec^{-1} to 120 mv dec^{-1}, while the cathodic Tafel slope shows a large variation, with rate of hydrogen evolution being high in the case of BA. Although the anodic polarization shows an active dissolution state to higher potentials in the case of PB and AP, their corrosion currents are low because the change in polarization was slow and the linear polarization resistance was high (Table 1). The passivation tendency seen in all these alloys except PB lies at a potential of 120 mV above E_{corr} and goes beyond 200 mV in case of AP.

Similar polarization experiments were carried out in other corrosive media using AP alloy: 1 N HCl and 5% NaCl (pH 5) (Fig. 6). The observed results (Table 3) show greater corrosion resistance in H_2SO_4 than in HCl. However, heat treatment of the alloys (AP and PB) show higher surface activity towards H_2SO_4 while lesser surface activity towards corrosive chloride media (Table 3). The passive behaviour of heat treated alloys (AP and PB) was also observed in these media.

Table 2
Corrosion data of the Ni–P alloys obtained under various bath compositions in 1 N H_2SO_4 at 303 K

Ni–P alloy	β_A (mV dec^{-1})	β_C (mV dec^{-1})	R_p (Ω)	i_{corr} (μA cm^{-2})	E_{corr} (mV)	C_{rate} (mpy)
PB	65	207	0.78	27.8	−34	12
AP	104	141	0.40	65.6	−278	81
NS[a]	60	219	0.16	127.4	−198	58
SC	114	143	0.15	180.8	−245	81
BA	55	440	0.19	113.8	−217	52
PL	57	293	0.51	40.6	−183	12

[a] NS unstirred AP bath.

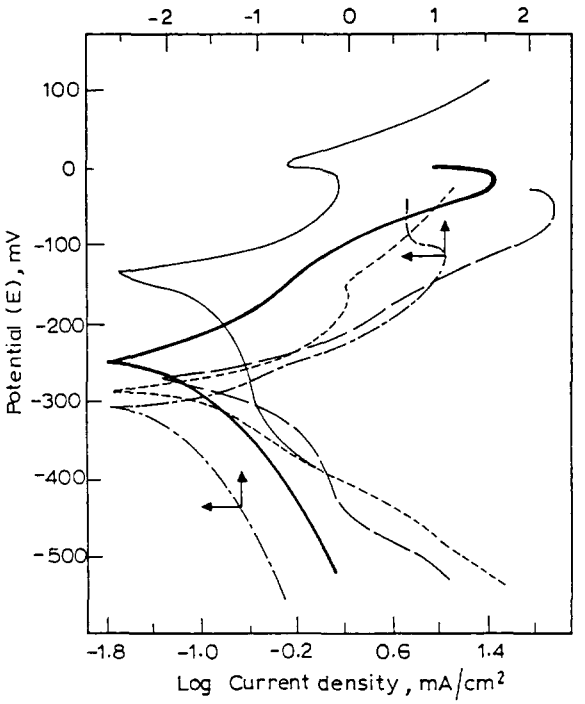

Fig. 6. Polarization patterns of the as-plated (AP) and heat-treated (APH) alloys in different media: (—) AP in 1 N H_2SO_4; (—) APH in 1 N H_2SO_4; (– –) AP in 1 N HCl; (– – –) APH in 1 N HCl; (– · –) AP in 5% NaCl.

4. Discussion

The XRD technique which gives information on the bulk property of the coating has been considered as one of the tools to investigate their chemical behaviour. In the XRD pattern, the broadening effects are attributed to two main factors: small crystallite size as well as deformation due to internal stress [15]. On comparing the results of the XRD with that of the polarization it is observed that the variation of corrosion rate with the percentage of phosphorus follows a reverse order of variation with the FWHM of the coatings (Fig. 7). In the case of PL, the FWHM is small showing greater crystallinity.

Among the coatings developed, PL and AP samples exhibited greater corrosion resistance in H_2SO_4. This could be attributed to a higher rate of deposition which results in thick coherent coatings. On observing the corrosion behaviour of PL and PB coatings, three principal factors — the degree of amorphous state, extent of internal stress and the percentage of phosphorus — appear to be operative in governing their reactivity. The combined effect of all these or the dominance of any one is responsible for the observed relationship between the chemical reactivity and XRD line broadening. However, the increase in corrosion resistance with the increase in phosphorus content [16] need not always be true and there are other factors which affect the corrosion behaviour of these alloys.

Table 3
Corrosion data of the Ni–P alloy in different acidic media at 303 K

Medium	β_A (mV dec^{-1})	β_C (mV dec^{-1})	R_p (Ω)	i_{corr} (μA cm^{-2})	E_{corr} (mV)	C_{rate} (mpy)
1 N H_2SO_4	104.3	141.9	0.40	65.6	−278	28
	(130)	(267)	(0.14)	(275)	(−117)	(119)
1 N HCl	112.0	332.9	0.14	254.1	−237	110
	(116)	(91)	(0.14)	(157)	(−264)	(68)
5% NaCl	54.8	147.8	0.61	28.3	−370	12
(pH 5)	(94)	(280)	(0.13)	(20)	(−194)	(9)
1 N H_2SO_4[a]	73	243	0.13	195	−219	83

[a] Corrosion data of heat treated Ni–P alloy (PB).
Values of corrosion data of heat treated Ni–P alloy (AP) are given in parentheses.

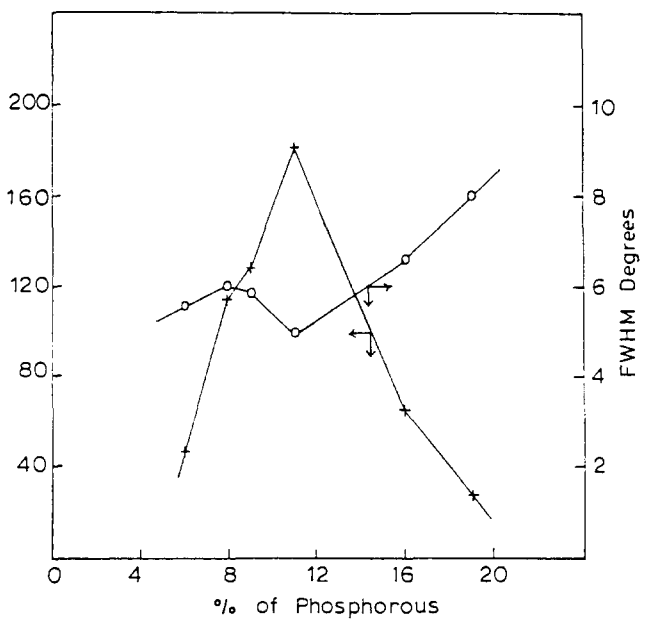

Fig. 7. Correlation of FWHM and i_{corr} in H_2SO_4 with the percentage of phosphorus.

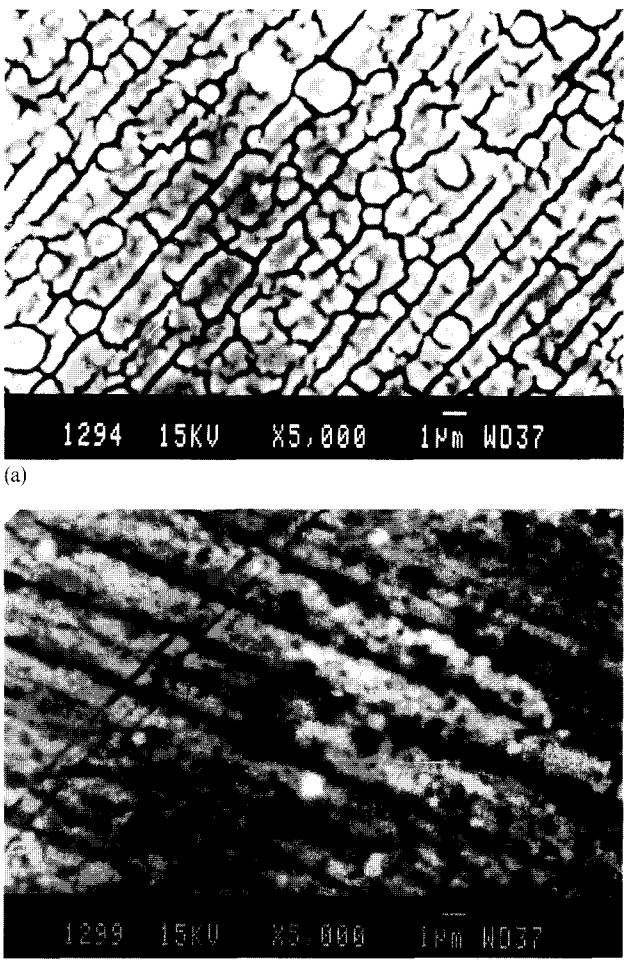

Fig. 8. Scanning electron microphotographs of the as-plated AP alloy after acid treatment: (A) H_2SO_4; (B) HCl.

The anodic Tafel slope values (50–120 mV dec^{-1}) show that the initial dissolution of the nickel metal goes through a monovalent intermediate state [17], followed by a passive state. Melendres and Pankuch [18] report the presence of $Ni(OH)_2$ and NiO in the passive film on nickel in the pH range 2.7–12, but the surface of the passive film of amorphous Ni–P alloys appears to be covered by a layer of adsorbed hypophosphite/phosphinate species which act as a protective layer [19]. The large variation in the cathodic Tafel slope in these coatings can be attributed to the surface inhibition by a passive film.

From the microscopic examination and corrosion measurements, it appears that these alloys exhibit an intrinsic intergranular attack with preferential growth along the boundary to form fissures in 1 N H_2SO_4 (Fig. 8A), while in HCl the dissolution of the blisters and smoothening of the roughness of the surface with pit formation (Fig. 8B) is observed. On heat treatment, the surface becomes relaxed owing to stress relief and hydrogen expulsion. Thus the stress corrosion in HCl will be less while the intergranular corrosion in H_2SO_4 will be more owing to the growth of the microcrystallites. This fact is further supported by the observed corrosion results (Table 3).

The surface of the PB alloy shows fewer blisters

(Fig. 1) than that of AP. It is likely that stabilizers such as lead ions become strongly adsorbed on the surface. Hydrogen overvoltage being high on lead, the number of blisters due to hydrogen embrittlement is less in PB. The difference in E_{corr} (Fig. 5, Table 2) for these coatings may be due to the differences in composition, thickness and porosity of the coating.

The observed experimental results such as dependence of structure and corrosion resistance on the plating conditions, increase in crystalline nature of the coating with heat treatment and dependence of chemical reactivity of coatings with composition on the amorphous state are in conformity with the earlier findings [20,21].

5. Conclusions

The correlation of microstructure with the corrosion behaviour is established with the plated Ni–P alloys. The formation of a new phase of Ni_5P_2 structurally distinguishes the BA and SC coatings from the others. The protective role of a stabilizer such as lead ions is significant and appears to be microscopically controlled. The synergistic action of boric acid and sodium chloride helps in increasing the corrosion resistance. The slight changes in the bath composition (stabilizer) bring a drastic change in the corrosion resistance. The rate of corrosion of PB and PL are much lower than those reported earlier.

6. Acknowledgements

The authors are grateful to the authorities of Bangalore University, Bangalore for providing research facilities. One of the authors (TM) thanks CSIR, New Delhi for a Senior Research Fellowship.

References

[1] M.F. Fernandez, J.M. Martinez-Duart and J.M. Albella, *Electrochim. Acta, 31* (1986) 55.
[2] J.F. Colaruotolo, *Plat. Surf. Finish, 121* (1985) 22.
[3] U. Hofmann and K.G. Weil, *Corros. Sci., 34* (1993) 423.
[4] G. Gutzeit and E.T. Mapp, *Corros. Technol., 3* (1956) 331.
[5] M.A. Trudgeon and J.R. Griffiths, *Br. Corros. J., 21* (1968) 331.
[6] J. Flis and D.J. Duquette, *Corrosion, 41* (1985) 700.
[7] K. Sugita and N. Veno, *J. Electrochem. Soc., 131* (1984) 111.
[8] W.J. Tomlinson and M.W. Carroll, *J. Mater. Sci., 25* (1990) 4972.
[9] R.B. Diegle, N.R. Sorensen and G.C. Nelson, *J. Electrochem. Soc., 133* (1986) 1769.
[10] T. Mimani and S.M. Mayanna, *Plat. Surf. Finish., 80* (1993) 66.
[11] M. Schlesinger, X. Meng and D.D. Snyder, *J. Electrochem. Soc., 138* (1991) 406.
[12] K.L. Lin, C.F. Yang and J.T. Lee, *Corrosion, 47* (1991) 17.
[13] B.E. Warren, *J. Appl. Phys., 12* (1941) 375.
[14] M. Henthorne, *Chem. Eng., July 26* (1971) 99.
[15] E.F. Kaelbe (ed.), Handbook of X-Rays, McGraw-Hill, New York, Part 2, 1967, p. 17.
[16] R.N. Duncan, *Plat. Surf. Finish., 7* (1986) 52.
[17] J.R. Vilche and A.J. Arvia, in R.P. Frankenthal and J. Kruger (eds.), Passivity of Metals, The Electrochemical Society, Princeton NJ, 1978, p. 681.
[18] C.A. Melendres and M. Pankuch, *J. Electroanal. Chem., 333* (1992) 103.
[19] R.B. Diegle, N.R. Sorensen, C.R. Clayton, M.A. Helfand and Y.C. Yu, *J. Electrochem. Soc., 135* (1988) 1085.
[20] A.T.El. Mallah, H. Hassib Abbas, M. Farid Shafei, M. El-Sayed Aboul Hassan and I. Nagi, *Plat. Surf. Finish., 5* (1989) 124.
[21] H. Habazaki, S.-Q. Ding, A. Kawashima, K. Asami, K. Hashimoto, A. Inoue and T. Masumoto, *Corros. Sci., 29* (1989) 1319.